6A.5 The Origins of Rotation within High-Shear, Low-CAPE Mesovortices and Mesocyclones

Keith D. Sherburn* and Matthew D. Parker
Department of Marine, Earth, and Atmospheric Sciences, North Carolina State University, Raleigh, North Carolina

ABSTRACT

A large fraction of eastern U.S. cool season and overnight tornadoes and significant straight-line wind events occur within high-shear, low-CAPE (HSLC) environments; however, this portion of the parameter space is also associated with low probability of detection and high false alarm rates of NWS watch and warning products. The compact spatial dimensions of HSLC mesovortices and mesocyclones (~2-4 km in diameter and depth) make their interrogation by radar challenging. Additionally, these sizes are comparable to the grid spacing of operational convection-allowing models, meaning that they are poorly (if at all) represented in high-resolution numerical weather prediction.

The purpose of this work is to evaluate high-resolution, idealized simulations of HSLC QLCSs in an attempt to elucidate the origins of rotation within these embedded mesovortices and mesocyclones. Data collected near HSLC convection during recent field projects, along with observed and modeled soundings from case studies and climatologies of severe HSLC convection, are used as a basis for the homogeneous, idealized environment in these simulations. In addition to process studies focused on the origins of rotation, sensitivity studies varying the vertical distributions of CAPE and shear are undertaken to determine what environmental characteristics promote versus curb the development of embedded supercells and mesovortices.

1. Introduction

Convection within high-shear, low-CAPE (HSLC) environments has been subject to rigorous investigation in the last decade. Much of this research has focused on producing a general climatology of severe HSLC convection and its associated synoptic-scale and mesoscale patterns (e.g., Schneider et al. 2006; Schneider and Dean 2008; Sherburn and Parker 2014; Sherburn et al. 2016). Further research has investigated the many operational considerations associated with HSLC convection, including: its tendency to occur during the cool season or overnight hours (e.g., Guyer at al. 2006; Smith et al. 2008); its relatively small spatial and temporal dimensions, leading to challenges in radar operations (e.g., Davis and Parker 2014); its relatively large fraction of quasi-linear convective system (QLCS) tornadoes (e.g., Thompson et al. 2012; Davis and Parker 2014); and the environments' apparent rapid destabilization preceding the arrival of convection, which may be unresolvable in conventional guidance (e.g., King and Parker 2015). Combined, these challenges contribute to low probability of detection and high false alarm rate of associated tornado watch and warning products issued by the National Weather Service (Dean and Schneider 2012; Anderson-Frey et al. 2016).

The aforementioned recent work has improved understanding of HSLC convection and discrimination between severe and non-severe HSLC convective events. However, as a result of very few targeted observations and numerical simulations of HSLC events, there remain many gaps in our knowledge regarding the dynamics that govern the differences between severe and non-severe convection. Additionally, prior HSLC simulations have largely focused on tropical mini-supercell environments (e.g., McCaul and Weisman 1996, 2001), which share a portion of the parameter space with the mid-latitude phenomenon discussed here. Studies investigating HSLC QLCS simulations have been limited in scope by presenting only one case (Wheatley and Trapp 2008) or performing largely qualitative comparisons (Sherburn and Parker 2015). As such, a general sensitivity study aimed to determine portions of the HSLC parameter space where strong low-level vortices can be expected had not been performed until now.

Recent research has elucidated the mechanisms by which low-level rotation originates in supercells within high-CAPE environments typical of the U.S. Great Plains (e.g., Markowski and Richardson 2014; Dahl et al. 2014), although there remains some debate regarding the relative contribution of various terms to low-level vertical vorticity, including baroclinic (e.g., Dahl 2015) and frictional (e.g., Schenkman et al. 2014; Markowski

[1]*Corresponding author address*: Keith Sherburn, Department of Marine, Earth, and Atmospheric Sciences, Campus Box 8208, North Carolina State University, Raleigh, NC 27695-8208; E-mail: kdsherbu@ncsu.edu

2016) generation. Via trajectory analysis, these studies have also identified the general pathways by which parcels approach and contribute to intense low-level vortices. Studies focused on the development of QLCS mesovortices have also been performed (Trapp and Weisman 2003; Weisman and Trapp 2003; Wheatley and Trapp 2008; Atkins and St. Laurent 2009a, b; Schenkman et al. 2012), though there is not a leading theory for their formation. Few similar studies have been performed for HSLC environments, be it with mini-supercell or QLCS convective modes. In addition to sensitivity tests of the parameter space, secondary aims of this work are to determine how strong low-level vortices form in HSLC environments and how these formation mechanisms differ, if at all, from higher-CAPE environments.

2. Data and Methods

a. Model sensitivity matrix

A seven-member model sensitivity matrix was developed to examine how variations in low- and mid-level shear vector magnitude and low-level (0-3 km) CAPE affect convective structure, evolution, and intensity. The control base-state environment is shown in Figure 1 and exhibits 493 J kg^{-1} of surface-based (SB) CAPE, 21 J kg^{-1} of 0-3 km CAPE, and 30 kt (1 kt = 0.51 m s^{-1}), 45 kt, and 83 kt of 0-1 km, 0-3 km, and 0-6 km shear vector magnitude, respectively. The control thermodynamic and kinematic profiles are based upon prior HSLC composites (e.g., Sherburn et al. 2016) and preliminary radiosonde data from the VORTEX-SE field experiment and HSLC-focused radiosonde launches from NC State University.

Table 1 shows the variability in chosen convective ingredients from the control base-state environment to the other six simulations. Note that changes in low-level CAPE do not alter the SBCAPE but do lead to minor differences in mixed-layer (ML) CAPE. Although not shown, the 0-1 km, 0-3 km, and 0-6 km shear vector orientations remain constant across all simulations. Storm-relative helicity (SRH) values change considerably with variations in shear vector magnitudes but also—perhaps unintuitively—change slightly with low-level CAPE due to the chosen storm motion estimate, which depends on the effective inflow base (Bunkers et al. 2014). Overall, this matrix represents the typical parameter space of HSLC convection fairly well, but future work will explore additional combinations of variables.

b. Model setup

Simulations were performed using the Bryan Cloud Model (CM1; e.g., Bryan and Fritsch 2002; Bryan and Rotunno 2009), release 18. Horizontal grid spacing in y was 250 m throughout the domain, and the north and south boundaries were periodic. The x grid was stretched from 250 m in the inner 100 km to 2 km at the model's east and west open boundaries. Note that the horizontal grid spacing here is fairly coarse given the scale of HSLC vortices (e.g., Davis and Parker 2014), and simulation results here are presented with the caveat that near-surface vortices are likely not entirely resolved.

The vertical grid spacing was stretched from 20 m in the lowest 1 km to 500 m from 7.5 km to the model top of 15 km. This included 50 levels in the lowest 1 km and a lowest model level of 10 m. A cold pool initialization was used, which was characterized by a minimum potential temperature perturbation of -10 K, decreasing as a cosine function eastward and upward from the western and bottom edge of the domain. The domain moved with a constant speed that varied slightly based upon the base-state environment to ensure that convection remained near the center of the domain within the unstretched x grid. Coriolis forcing was included on the perturbation winds only, which is equivalent to assuming geostrophic balance in the base-state wind field (Roberts et al. 2016; Coffer and Parker 2016). The simulations were initialized with modest, random potential temperature perturbations throughout the domain to encourage more rapid development of three-dimensional convective structures. The NSSL double-moment microphysics scheme is used, with both graupel and hail densities predicted. The bottom boundary is free-slip, and surface fluxes and radiation are excluded for simplicity.

c. Parcels and trajectories

For each simulation that produced a relatively strong vortex, a restart run was performed in which tracer parcels were seeded within the model. Parcels were initiated at each grid point within a 50 km (in x) by 100 km (in y) by 1.4 km (in z) box ahead, and in the vicinity, of the location where the strongest 10-m vortex developed. Candidate parcels were then filtered by maximum low-level vertical vorticity to determine the origins and forward trajectories of parcels that eventually contributed to strong low-level vortices. Although near-surface vortices were the primary point of investigation for this work, future research will investigate the origins of rotating updrafts, or embedded mesocyclones, within HSLC QLCS simulations. Parcel trajectories were calculated at every large model time step, with output written every ten seconds.

3. Preliminary Results

a. Overview

Convection was rather slow to develop in all simulations, with initial convective updrafts generally emerging in the 100-150 min time period. Following initiation, convection in each simulation evolved from primarily scattered cells to a QLCS mode, with many simulations exhibiting at least transient embedded supercellular features. These embedded supercells, which exhibited realistic simulated reflectivity structures (Fig. 4) and considerable updraft helicity (Fig. 5), had life cycles ranging from approximately 30 to 90 min. Most simulations also eventually produced strong low-level vortices with maximum surface vertical vorticity surpassing 0.1 s^{-1}. Curiously, these low-level vortices—particularly when weakening—tended to move to the right of the embedded mesocyclones (sometimes by as much as 90 degrees, see Fig. 6). Maximum values for 1-km vertical velocity, 1-km vertical vorticity, 10-m vertical vorticity, and 10-m wind speed[2] are provided in Table 2 for comparison between the seven runs.

b. Low-level shear vector magnitude sensitivity

Compared to the other variables, low-level shear vector magnitude appeared to have the most substantial impact on the potential for simulated convection to produce strong low-level vortices. Additionally, decreasing the low-level shear vector magnitude essentially eradicated the presence of embedded supercellular features. These two sensitivities are likely not independent of one another; in particular, it is speculated that the stronger dynamic forcing for ascent via the vertical perturbation pressure gradient acceleration into mid-level vortices subsequently enhanced tilting of low-level horizontal vorticity and stretching of low-level vertical vorticity, as has been documented in many prior studies. This would imply a relationship between the low-level shear vector magnitude and low-to-mid-level updraft rotation, which is consistent with existing theory.

At any rate, the simulation with decreased low-level shear vector magnitude (-LLshear) generally produced the weakest simulated convection within the matrix, with no strong low-level vortices observed. Convection within the increased low-level shear vector magnitude simulation (+LLshear) was among the strongest in the matrix, particularly in the first 180 min. The strongest near-surface vortices in the matrix were also observed in +LLshear. These findings are generally consistent with the mesovortex studies of Weisman and Trapp (2003) and Atkins and St. Laurent (2009a). Additionally, these findings corroborate the parameter-based work of Sherburn et al. (2016), who showed that shear vector magnitudes over shallow layers (in particular, 0-1.5 km) were useful in discriminating between severe and nonsevere HSLC environments.

c. Mid-level shear vector magnitude sensitivity

Modifying the mid-level shear vector magnitude appeared to primarily influence the *location* of convective development and evolution. With increased mid-level shear vector magnitude (+MLshear), convection developed well ahead of the initiating cold pool and subsequently evolved along its own, system-generated cold pool. On the contrary, convection in the decreased mid-level shear vector magnitude simulation (-MLshear) developed close to the initiating cold pool and subsequently evolved along this boundary.

The simulated convection's proximity to this initial cold pool led to noteworthy changes in its structure and associated low-level vortices. In particular, convection in +MLshear began as scattered mini-supercells before growing upscale into a convective system as it weakened, whereas convection in -MLshear rapidly evolved into a QLCS. The quasi-isolated mini-supercells in +MLshear ultimately supported the strongest low-level vortices in this particular run, which superficially appeared to develop in a manner and location similar to higher-CAPE supercells. Within

[2] Note that 10-m wind speeds are likely overestimated due to the free-slip lower boundary condition.

-MLshear, several vortices developed along the leading edge of the cold pool, appearing to strengthen as they encountered overlying updrafts. There are some indications that these vortices arise from the development of a vortex sheet along the cold pool's leading edge, particularly given their fairly regular spacing. This will be explored further in future work.

d. Low-level CAPE sensitivity

The magnitude of low-level CAPE appears to primarily influence the convective time scale. In other words, the base-state with increased low-level CAPE (+LLCAPE) produced convection earlier in the simulation that subsequently reached its peak strength earlier in the simulation. Meanwhile, the decreased low-level CAPE simulation (-LLCAPE) produced slower convective development and evolution. Eventually, the two simulations are comparable, with each producing QLCS structures and embedded supercellular elements. Quantitative metrics, such as maximum updraft speeds and near-surface vertical vorticity, are also generally comparable between the two.

e. Trajectory analysis

Thus far, trajectory analysis has primarily focused on +LLshr and +LLCAPE. Both simulations produced strong near-surface vortices, with 10-m vertical vorticity greater than 0.1 s^{-1} and Okubo-Weiss parameter (Okubo 1970; Weiss 1991)[3] values over 0.05 s^{-2}. However, the convective mode during the time of these vortices varied between the runs, with embedded supercells apparent in +LLCAPE and a dominant QLCS mode observed in +LLshr.

The pathways by which parcels acquired appreciable (0.025 s^{-1}) near-surface ($z = 10$ m) vertical vorticity in +LLCAPE were rather straightforward and generally "traditional" when compared to prior research on higher-CAPE supercells (Fig. 7). Namely, all parcels approached from the storm's northwest quadrant with little to no vertical motion, though some appear to take an "up-down" trajectory over an outflow boundary beforehand. Parcels appear to acquire appreciable vertical vorticity at 10-m during ascent and/or coincident with a horizontal left turn towards the location of vortex development, rather than descent. Further, much of the development of vertical vorticity occurs below the bottom model level.

In contrast, parcels acquiring appreciable vorticity at the bottom model level in +LLshr arrived from four different source regions (labeled "1", "2a", "2b", and "3" in Fig. 8). Initial parcels acquiring appreciable vertical vorticity arrived from storm-relative north (Fig. 8, annotated source region "1"). Subsequent parcels originated in the other three regions, though some pathways to the vortex ("2a" and "2b") were ultimately similar. As in +LLCAPE, parcels either attained vertical vorticity while taking a "left turn" towards the location of vortex development or during ascent; parcels entering the vortex did not acquire appreciable positive vertical vorticity during descent. These trajectories suggest that the source region of parcels acquiring large low-level vertical vorticity and contributing to strong near-surface vortices could—and likely do—change based upon the time they enter the vortex.

One final interesting note is that all parcels entering the vortex in +LLshr did so with *positive* buoyancy (Fig. 8, bottom right). This is counterintuitive based on conventional reasoning that near-surface vertical vorticity arises in association with a convective downdraft, which would tend to be cool relative to its surroundings. Additionally, all parcels entering the strongest vortex in +LLCAPE arrived with *negative* buoyancy (Fig. 8, bottom right), consistent with existing theory. This suggests the potential that the thermodynamics of parcels entering strong low-level vortices could vary based upon base state or convective mode. Future work will examine the differences in parcel characteristics and pathways between these two simulations (and others) in further detail.

4. Discussion and Conclusions

Preliminary results suggest that HSLC convection has the following sensitivities to environmental conditions:

- The low-level shear vector magnitude can help determine if strong, low-level vortices should be expected within HSLC convection. Larger values are conducive to the development of strong, low-level

[3] The Okubo-Weiss parameter is sometimes preferred over vertical vorticity because it effectively removes deformation from vertical vorticity, thus providing a focus on the location where rotation is dominant.

vortices, while simulations with weak low-level shear do not produce vortices of similar intensity. These findings are consistent with prior QLCS mesovortex studies (Weisman and Trapp 2003; Atkins and St. Laurent 2009a).

- Low-level shear vector magnitude also influences convective mode. Simulations with weak low-level shear do not support embedded supercells.
- Mid-level shear vector magnitude influences the location of convective development and evolution. Increased mid-level shear supports convective development ahead of an initial cold pool, with subsequent evolution along a system-generated cold pool. Decreased mid-level shear leads to convective development and evolution along the initiating boundary.
- Low-level CAPE plays a role in the convective time scale of simulated HSLC convection. Increased low-level CAPE leads to more rapid development and evolution of convection, though ultimate convective structure appears similar regardless of low-level CAPE.

While rigorous quantitative investigation into these sensitivities has yet to be conducted, we can speculate on their associated dynamics.

Increased low-level shear would lead to enhanced streamwise horizontal vorticity that could be tilted and stretched into the vertical. This, in turn, would be supportive of stronger mesocyclones, thus enhancing low-level vertical ascent. Subsequently, this ascent would be supportive of increased tilting of near-surface horizontal vorticity and stretching of near-surface vertical vorticity, contributing to stronger low-level vortices. These speculations are generally consistent with the suggestions of Markowski et al. (2012), among others. It is noted that within our prior climatological investigations, the most skillful value of 0-1 km shear vector magnitude in discriminating between severe and non-severe convective environments is approximately 31-33 kt, which is comparable to our control value of 30 kt. This implies that our -LLshr simulation is within the “less favorable” regime and +LLshr is “more favorable” based upon HSLC climatology.

In terms of the remaining variables, the impact of mid-level shear vector magnitude on location of convective development is a bit more obscure and will require further investigation. However, it is rather intuitive that increased CAPE would lead to more rapid development and evolution of convection. With that said, there are likely some nuances associated with this sensitivity that will be uncovered with more rigorous investigation. Additionally, it is worth exploring how an environment with little to no low-level CAPE can support embedded supercells.

Future work will examine these simulations in more quantitative detail, including a decomposition of the diagnostic perturbation pressure gradient acceleration and an assessment of the origins of vorticity within embedded mesocyclones. Furthermore, we plan to expand our matrix of simulations to encompass a broader portion of the parameter space in an effort to test the applicability and validity of our preliminary findings.

Preliminary trajectory analyses suggest that the pathways by which parcels acquire large near-surface vertical vorticity may be sensitive to the environmental base state and the time at which they enter low-level vortices. Additional trajectory analysis will be undertaken for the remaining simulations of the matrix to determine the representativeness of the trajectories shown here. Ongoing work seeks to calculate vorticity budgets along trajectories entering low-level vortices to determine the sources of rotation and how these differ from higher-CAPE vortices. It should be reiterated that given the horizontal grid spacing of these simulations, low-level vortices are, at best, marginally resolved. Thus, future work will also examine the potential of conducting these simulations at finer horizontal grid spacings to more adequately resolve the vortices of interest.

ACKNOWLEDGEMENTS

The authors are grateful to George Bryan for his development and support of CM1. We would also like to thank current and past members of the NC State Convective Storms Group for thought-provoking discussions on the research presented here. Additionally, we would like to thank the developers of SHARPpy for maintaining software used in this study to display and compare soundings. Finally, we acknowledge NOAA grant NA14NWS4680013, part of the Collaborative Science, Technology, and Applied Research program, which funded this research.

REFERENCES

Anderson-Frey, A., Y. P. Richardson, A. R. Dean, R. L. Thompson, and B. T. Smith, 2016: Investigation of tornado warning skill by environment. *Wea. Forecasting*, **31**, 1771-1790.

Atkins, N. T., and M. St. Laurent, 2009a: Bow Echo Mesovortices. Part I: Processes That Influence Their Damaging Potential. *Mon. Wea. Rev.*, **137**, 1497-1513.

Atkins, N. T., and M. St. Laurent, 2009b: Bow Echo Mesovortices. Part II: Their Genesis. *Mon. Wea. Rev.*, **137**, 1514-1532.

Bryan, G. H., J. M. Fritsch, 2002: A Benchmark Simulation for Moist Nonhydrostatic Numerical Models. *Mon. Wea. Rev.*, **130**, 2917-2928.

Bryan, G. H., and R. Rotunno, 2009: Evaluation of an Analytical Model for the Maximum Intensity of Tropical Cyclones. *J. Atmos. Sci.*, **66**, 3042-3060.

Bunkers, M. J., D. A. Barber, R. L. Thompson, R. Edwards, and J. Garner, 2014: Choosing a Universal Mean Wind for Supercell Motion Prediction. *J. Operational Meteor.*, **2** (11), 115-129.

Coffer, B. E., and M. D. Parker, 2016: Simulated supercells in nontornadic and tornadic VORTEX2 environments. *Mon. Wea. Rev.*, in press.

Dahl, J. M. L., 2015: Near-Ground Rotation in Simulated Supercells: On the Robustness of the Baroclinic Mechanism. *Mon. Wea. Rev.*, **143**, 4929-4942.

Dahl, J. M. L., M. D. Parker, and L. J. Wicker, 2014: Imported and Storm-Generated Near-Ground Vertical Vorticity in a Simulated Supercell. *J. Atmos. Sci.,* **71**, 3027-3051.

Davis, J. M., and M. D. Parker, 2014: Radar climatology of tornadic and non-tornadic vortices in high shear, low CAPE environments in the mid-Atlantic and southeastern U.S. *Wea. Forecasting*, **29**, 828-853.

Dean, A. R., and R. S. Schneider, 2012: An examination of tornado environments, events, and impacts from 2003-2012. Preprints, *26th Conf. on Severe Local Storms*, Nashville, TN, Amer. Meteor. Soc., P6.0.

Guyer, J. L., D. A. Imy, A. Kis, and K. Venable, 2006: Cool season significant (F2-F5) tornadoes in the Gulf Coast states. Preprints, *23rd Conf. on Severe Local Storms,* St. Louis, MO, Amer. Meteor. Soc., 4.2. [Available online at https://ams.confex.com/ams/pdfpapers/115320.pdf.]

King. J. R., and M. D. Parker, 2015: Conditioning and evolution of high shear, low CAPE environments. Preprints, *16th Conf. on Mesoscale Processes*, Boston, MA, Amer. Meteor. Soc.

Markowski, P. M., 2016: An Idealized Numerical Simulation Investigation of the Effects of Surface Drag on the Development of Near-Surface Vertical Vorticity in Supercell Thunderstorms. *J. Atmos. Sci.*, **73**, 4349-4385.

Markowski, P. M., and Y. P. Richardson, 2014: The Influence of Environmental Low-Level Shear and Cold Pools on Tornadogenesis: Insights from Idealized Simulations. *J. Atmos. Sci.*, **71**, 243-275.

Markowski, P., Y. Richardson, J. Marquis, R. Davies-Jones, J. Wurman, K. Kosiba, P. Robinson, E. Rasmussen, and D. Dowell, 2012: The Pretornadic Phase of the Goshen County, Wyoming, Supercell of 5 June 2009 Intercepted by VORTEX2. Part II: Intensification of Low-Level Rotation. *Mon. Wea. Rev.*, **140**, 2916-2938.

McCaul, E. W., Jr., and M. L. Weisman, 1996: Simulation of shallow supercell storms in landfalling hurricane environments. *Mon. Wea. Rev.*, **124**, 408-429.

McCaul, E. W., Jr., and M. L. Weisman, 2001: The sensitivity of simulated supercell structure and intensity to variations in the shapes of environmental buoyancy and shear profiles. *Mon. Wea. Rev.*, **129**, 664-687.

Okubo, A., 1970: Horizontal dispersion of floatable particles in the vicinity of velocity singularities such as convergences. *Deep-Sea Res.*, **17**, 445-454.

Roberts, B., M. Xue, A. D. Schenkman, and D. T. Dawson II, 2016: The Role of Surface Drag in Tornadogenesis within an Idealized Supercell Simulation. *J. Atmos. Sci.*, **73**, 3371-3395.

Schenkman, A. D., M. Xue, and A. Shapiro, 2012: Tornadogenesis in a Simulated Mesovortex within a Mesoscale Convective System. *J. Atmos. Sci.*, **69**, 3372-3390.

Schenkman, A. D., M. Xue, and M. Hu, 2014: Tornadogenesis in a High-Resolution Simulation of the 8 May 2003 Oklahoma City Supercell. *J. Atmos. Sci.*, **71**, 130-154.

Schneider, R. S., A. R. Dean, S. J. Weiss, and P. D. Bothwell, 2006: Analysis of estimated environments for 2004 and 2005 severe convective storm reports. Preprints, *23rd Conf. on Severe Local Storms*, St. Louis, MO, Amer. Meteor. Soc., 3.5. [Available online at https://ams.confex.com/ams/pdfpapers/115246.pdf.]

Schneider, R. S., and A. R. Dean, 2008: A comprehensive 5-year severe storm environment climatology for the continental United States. Preprints, *24th Conf. on Severe Local Storms,* Savannah, GA, Amer. Meteor. Soc., 16A.4. [Available online at https://ams.confex.com/ams/pdfpapers/141748.pdf.]

Sherburn, K. D., and M. D. Parker, 2014: Climatology and ingredients of significant severe convection in high-shear, low-CAPE environments. *Wea. Forecasting,* **29**, 854-877.

Sherburn, K. D., and M. D. Parker, 2015: Examining the sensitivities of high-shear low-CAPE convective to low-level hodograph shape. Preprints, *16th Conf. on Mesoscale Processes*, Boston, MA, Amer. Meteor. Soc.

Sherburn, K. D., M. D. Parker, J. R. King, and G. M. Lackmann, 2016: Composite environments of severe and non-severe high-shear, low-CAPE convective events. *Wea. Forecasting*, **31**, 1899-1927.

Smith, B. T., J. L. Guyer, and A. R. Dean, 2008: The climatology, convective mode, and mesoscale environment of cool season severe thunderstorms in the Ohio and Tennessee Valleys, 1995–2006. Preprints, *24th Conf. on Severe Local Storms,* Savannah, GA, Amer. Meteor. Soc., 13B.7. [Available online at https://ams.confex.com/ams/pdfpapers/141968.pdf.]

Thompson, R. L., B. T. Smith, J. S. Grams, A. R. Dean, and C. Broyles, 2012: Convective modes for significant severe thunderstorms in the contiguous United States. Part II: Supercell and QLCS environments. *Wea. Forecasting*, **27**, 1114-1135.

Trapp, R. J., and M. L. Weisman, 2003: Low-Level Mesovortices within Squall Lines and Bow Echoes. Part II: Their Genesis and Implications. *Mon. Wea. Rev.*, **131**, 2804-2823.

Weisman, M. L., and R. J. Trapp, 2003: Low-Level Mesovortices within Squall Lines and Bow Echoes. Part I: Overview and Dependence on Environmental Shear. *Mon. Wea. Rev.*, **131**, 2779-2803.

Weiss, J., 1991: The dynamics of enstrophy transfer in two-dimensional hydrodynamics. *Physica D*, **48**, 273-294.

Wheatley, D. M., and R. J. Trapp, 2008: The Effect of Mesoscale Heterogeneity on the Genesis and Structure of Mesovortices within Quasi-Linear Convective Systems. *Mon. Wea. Rev.*, **136**, 4220-4241.

Table 1. Selected base-state environment variables for matrix of simulations

Variable	**Control**	**+LLshear**	**-LLshear**	**+MLshear**	**-MLshear**	**+LLCAPE**	**-LLCAPE**
SBCAPE (J kg^{-1})	493	493	493	493	493	493	493
MLCAPE (J kg^{-1})	274	274	274	274	274	276	288
0-3 km CAPE (J kg^{-1})	21	21	21	21	21	40	6
0-1 km shear (kt)	30	40	20	30	30	30	30
0-1 km SRH (m^{2}s^{-2})	253	352	160	271	233	236	264
0-3 km shear (kt)	45	45	45	54	35	45	45
0-3 km SRH (m^{2}s^{-2})	369	451	304	448	300	366	370
0-6 km shear (kt)	83	83	83	93	73	83	83

Table 2. Selected quantitative characteristics for matrix of simulations. Maximum value within the matrix of seven simulations is bolded and italicized.

Variable	**Control**	**+LLshear**	**-LLshear**	**+MLshear**	**-MLshear**	**+LLCAPE**	**-LLCAPE**
Maximum w (m s^{-1})	36.18	33.59	35.09	33.33	33.19	31.32	***36.92***
Maximum 10-m ζ (s^{-1})	0.144	***0.245***	0.078	0.189	0.214	0.187	0.170
Maximum 1-km ζ (s^{-1})	0.087	0.101	0.071	0.120	***0.153***	0.109	0.100
Maximum 10-m wind speed (m s^{-1})	55.23	***60.30***	35.50	52.83	58.39	52.93	48.10

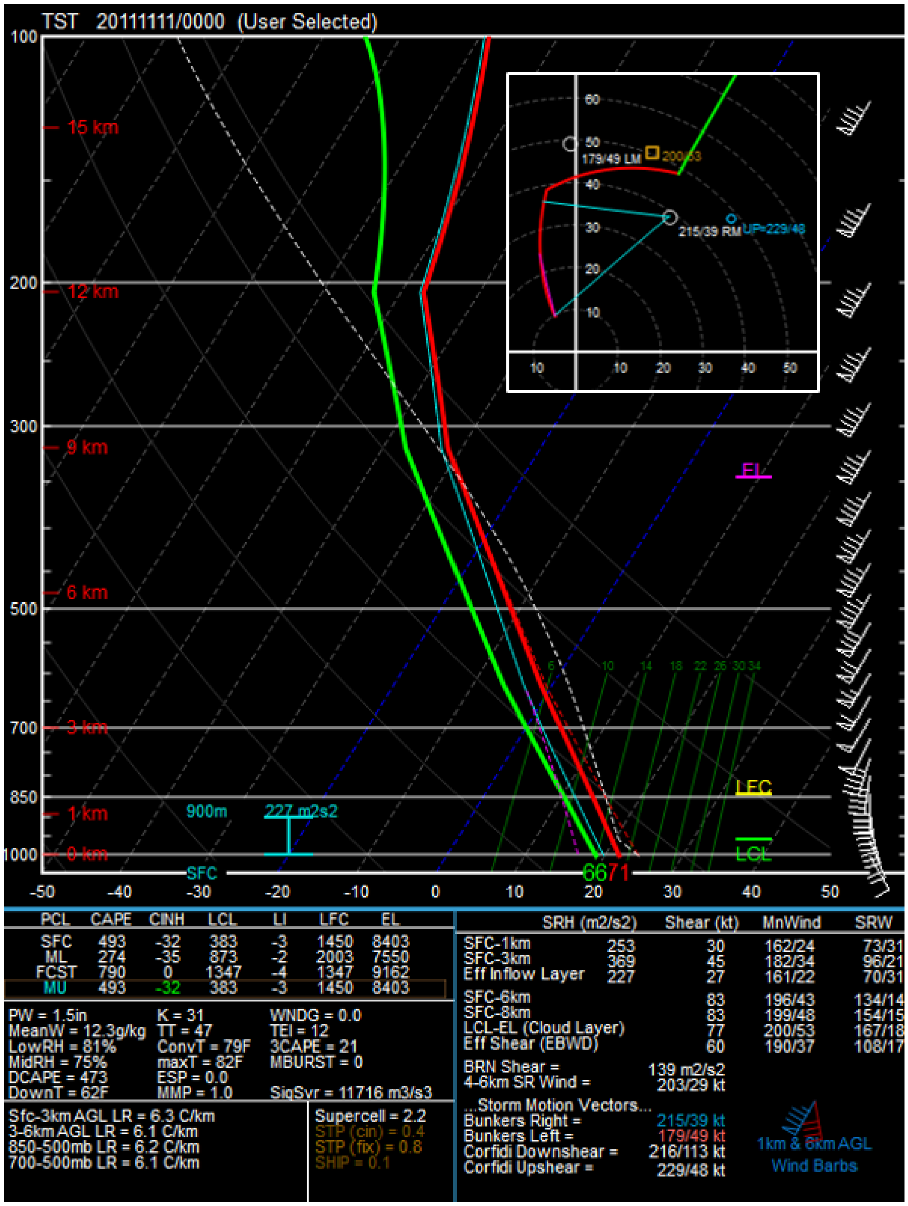

Figure 1. Control base-state environment in HSLC matrix of simulations.

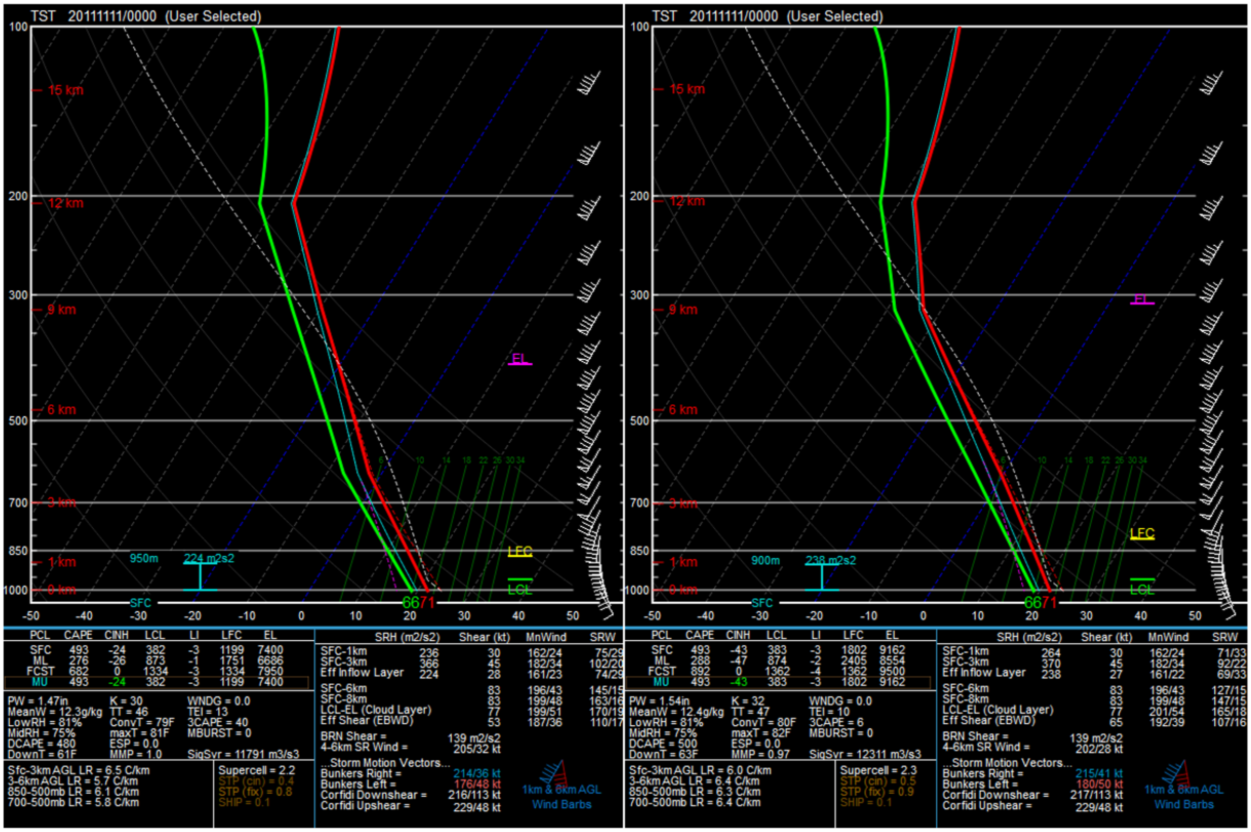

Figure 2. Base-state thermodynamic profiles for the (left) increased low-level CAPE and (right) decreased low-level CAPE simulations.

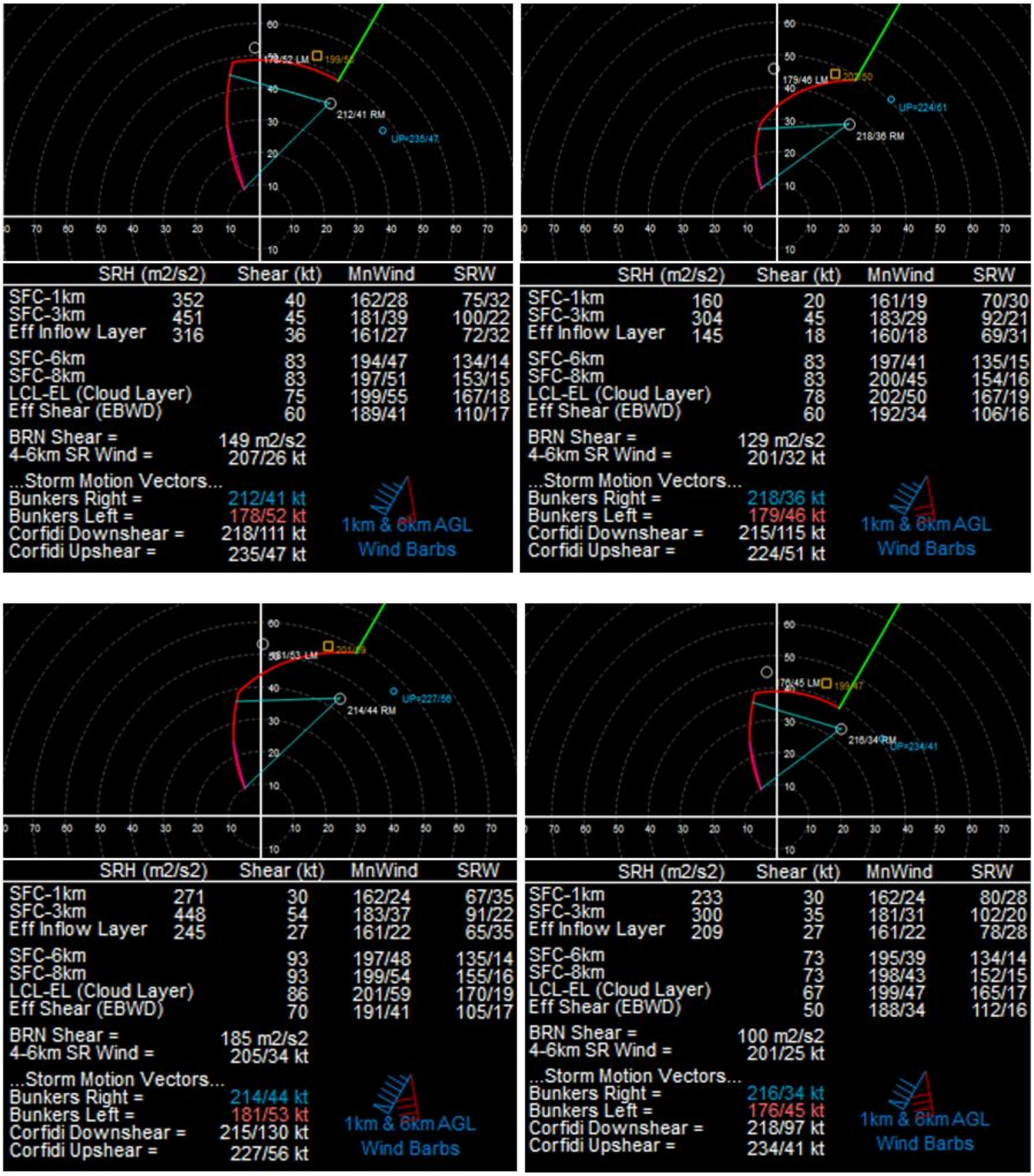

Figure 3. Base-state kinematic profiles for the (left) increased (top) low-level shear vector magnitude and (bottom) mid-level shear vector magnitude and (right) decreased low-level and mid-level shear vector magnitudes (top and bottom, respectively).

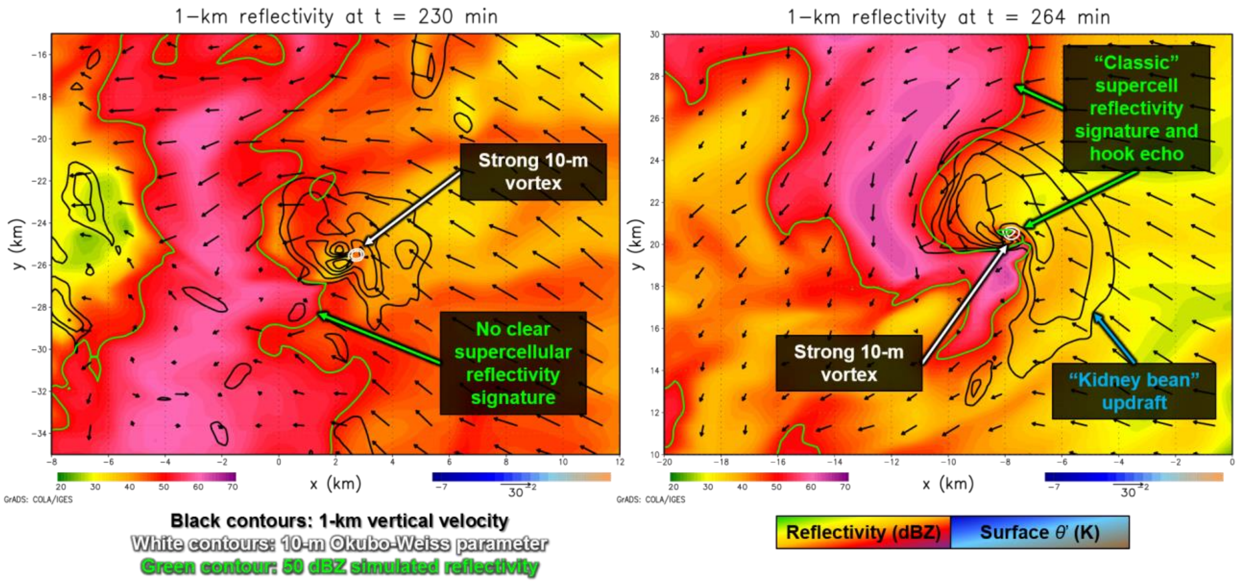

Figure 4. Snapshots of simulated reflectivity (dBZ, shaded), 1-km vertical velocity (m s^{-1}, black contours), 10-m Okubo-Weiss parameter (s^{-2}, white contours), and the 50 dBZ contour (green) from the increased low-level shear vector magnitude simulation (left) and the increased low-level CAPE simulation (right) at time of strongest near-surface vortex. Note the QLCS reflectivity structure on the left and classic supercell-esque reflectivity structure on the right, along with a corresponding typical kidney bean shaped updraft.

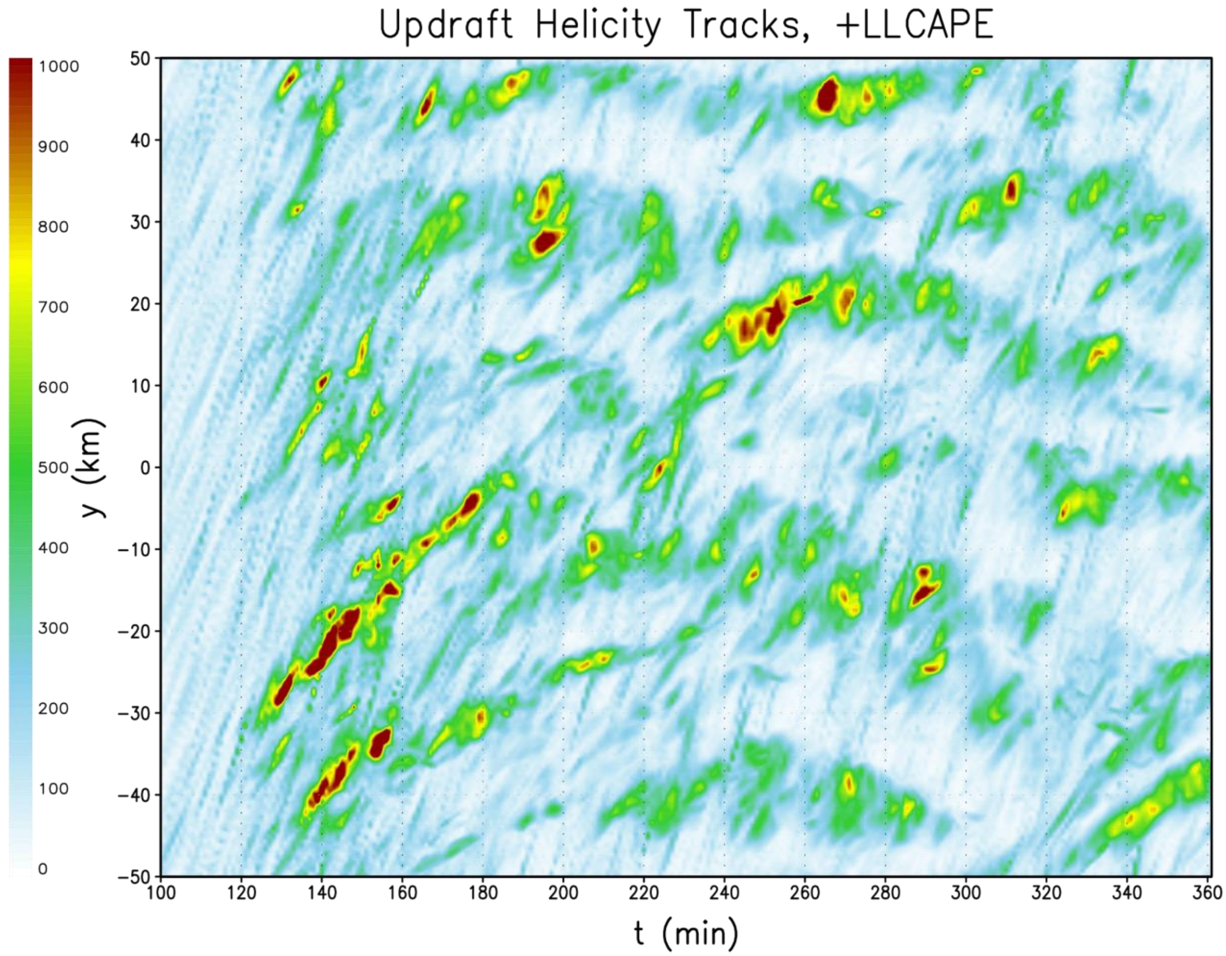

Figure 5. Longitudinal maximum updraft helicity ($m^2\ s^{-2}$) Hovmoller diagram for the increased low-level CAPE simulation, with time on the abscissa and y on the ordinate. Continuous tracks of enhanced updraft helicity indicate embedded supercellular features within the broader QLCS.

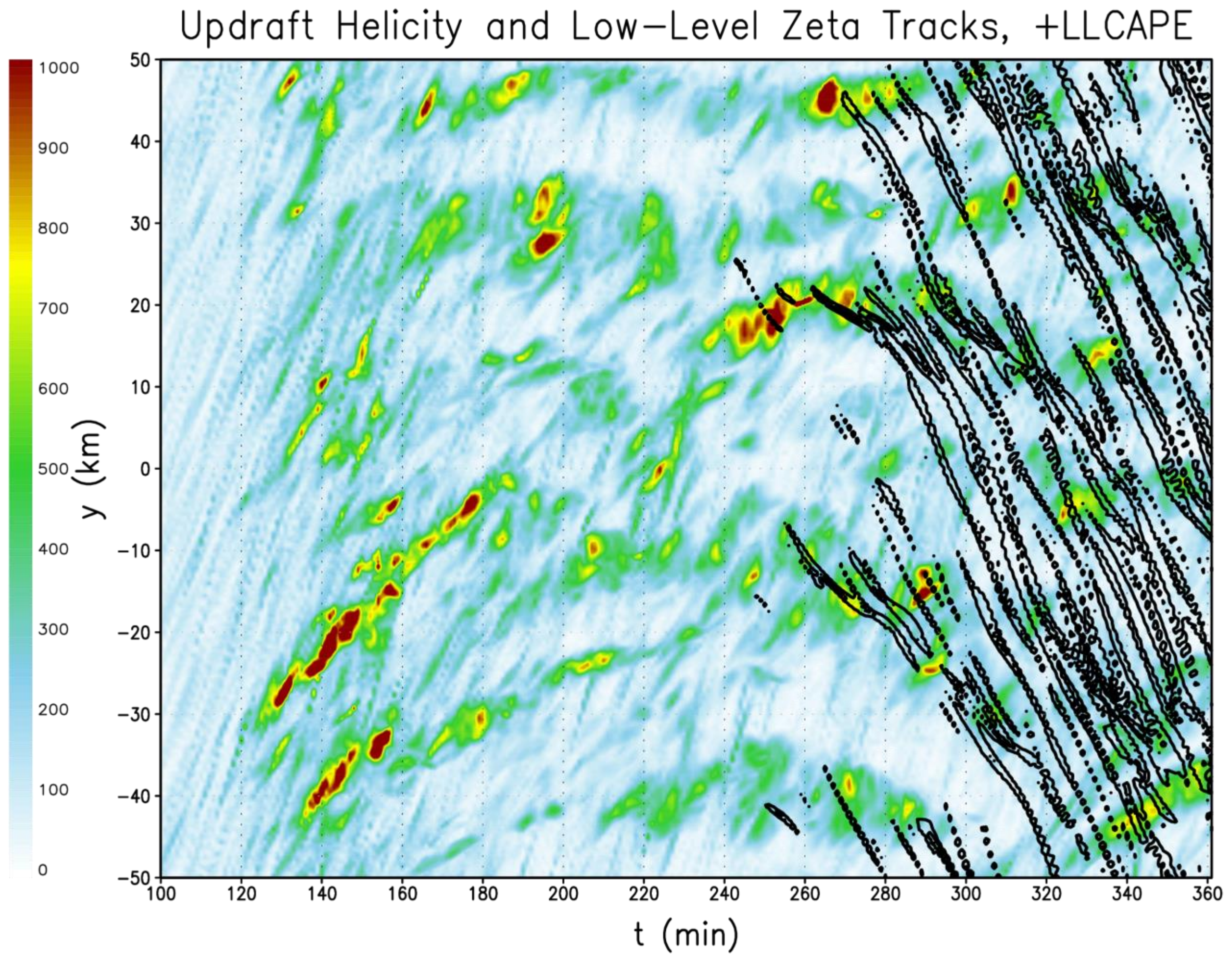

Figure 6. As in Fig. 5, but including 10-m vertical vorticity (s^{-1}, black contours) tracks. Note that vertical vorticity maxima appear to have a motion vector approximately 45 to 90 degrees to the right of the dominant mesocyclone tracks.

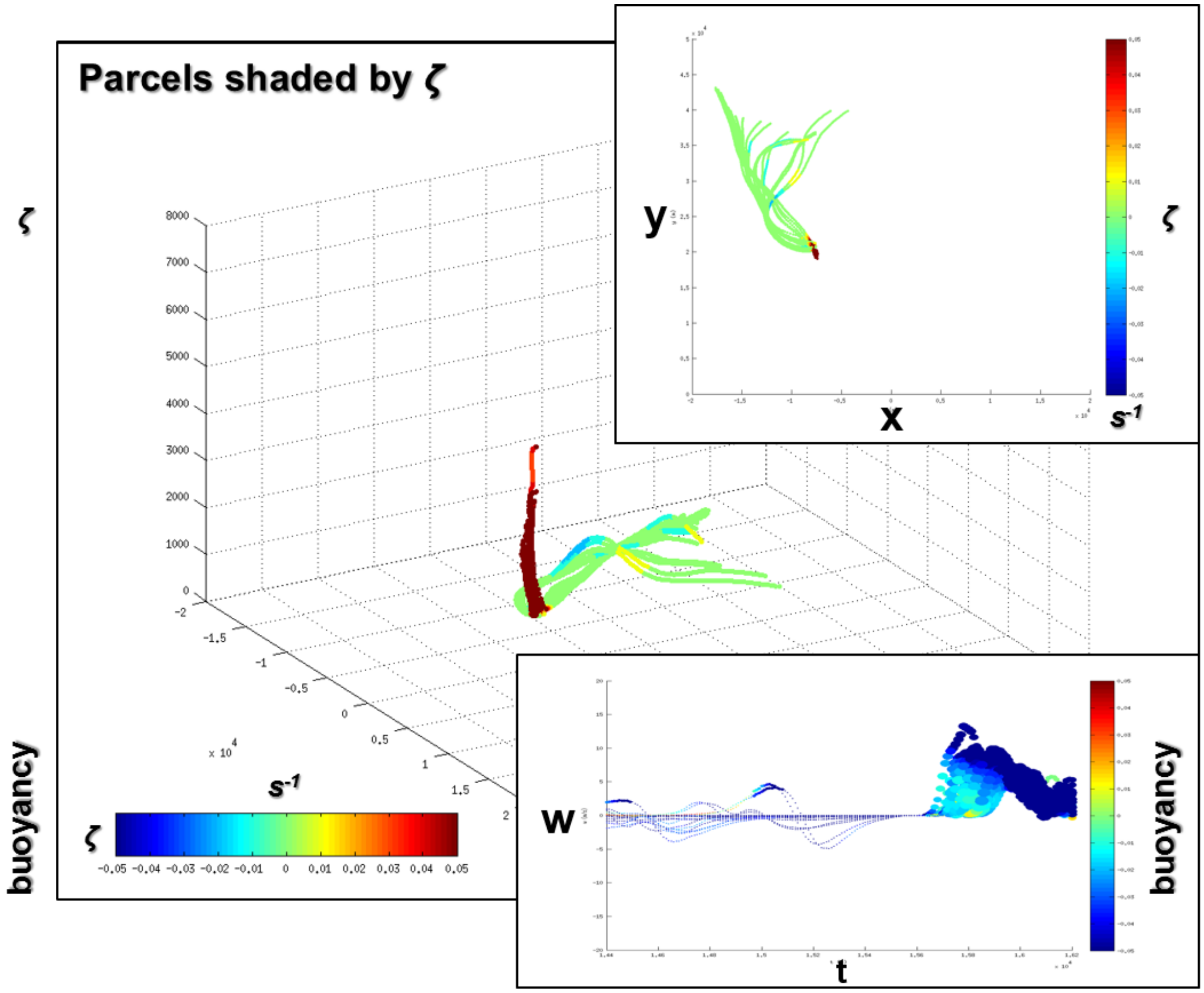

Figure 7. Trajectories of parcels acquiring at least 0.025 s^{-1} of 10-m vertical vorticity during the time of strongest near-surface vortex development in the increased low-level CAPE simulation. Large panel shows a three-dimensional rendering of these trajectories, shaded by 10-m vertical vorticity (s^{-1}). Top right panel shows the same but in a plan-view, x-y domain. The bottom right panel shows a time versus vertical velocity plot, with parcels shaded by their buoyancy ($m^2\ s^{-1}$) and sized based upon their vertical vorticity.

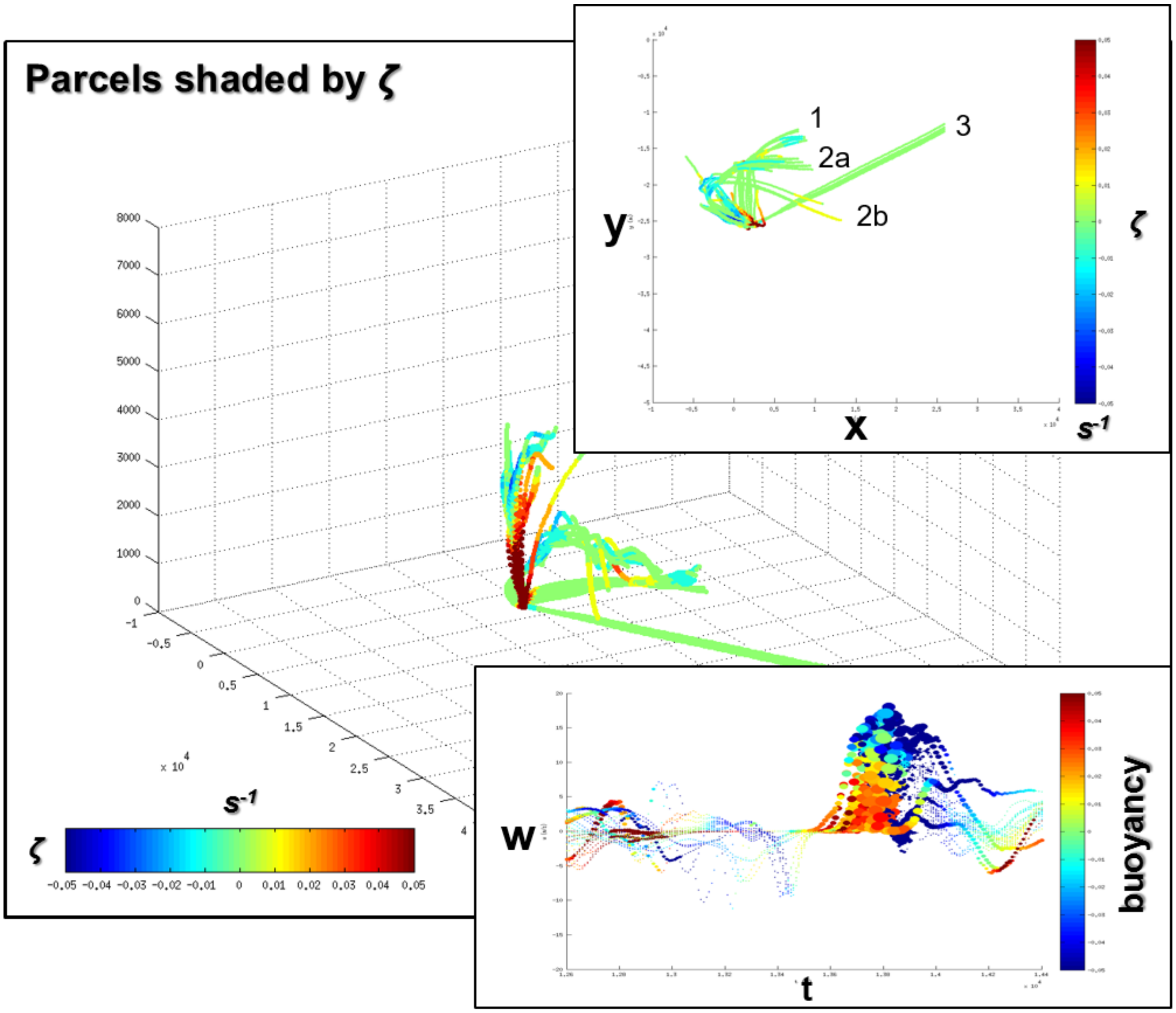

Figure 8. As in Fig. 7, but for the increased low-level shear vector magnitude simulation. Source regions referred to in the text are annotated in the top right panel.